Approximate treatment of the continuum

T. Vertse
Institute of Nuclear Research of the Hungarian Academy of Sciences, H-4001 Debrecen, Pf. 51, Hungary

P. Curutchet and R. J. Liotta
Research Institute of Physics, S-10405 Stockholm, Sweden
(Received 25 April 1990)

Pole expansions of the Green function (Berggren and Mittag-Leffler) are used to calculate single-particle and particle-hole response functions for a square well plus Coulomb potential and the results are compared with the corresponding exact ones. The approximate and exact response functions agree well with each other in the resonant energy region. The Mittag-Leffler expansion is shown to be valid even for the long-range Coulomb potential. The computation time needed for the calculation of the particle-hole response function can be reduced considerably by using the pole expansions.

I. INTRODUCTION

Currently, a considerable amount of attention is being devoted to the study of the particle decay of giant resonances.[1-6] Both the theoretical and the experimental analyses of the problem present formidable difficulties.[1-4] From the theoretical point of view, the main complication is to include the contribution of the continuum in the building up of the giant resonances. To overcome this difficulty an approximate method called the resonant random-phase approximation (RRPA) was recently developed.[5,6] In the RRPA the single-particle Green function is expanded in a basis composed of bound single-particle states and single-particle-resonant (Gamow) states.[7] The use of Gamow states automatically takes care of the possibility of particle emission from the unbound particle states. The advantage of the RRPA is that it deals only with discrete eigenstates, therefore methods well known from nuclear structure calculations can still be used. The price one pays for this convenience is that the RRPA is an approximate method. Yet, the calculated quantities agree well with available experimental data. As a test of the RRPA, we reproduced cases[5] where the effect of the continuum was taken into account exactly.[8,9] That comparison only tested the method in a qualitative way either because of uncertainties related to the extraction of parameters or because the parameters included in the calculations were not always fully specified.

In order to perform a quantitative test of the approximations leading to the RRPA without the influence of the disturbing aforementioned factors we will perform in this paper calculations of single-particle and particle-hole response functions both in exact and approximate ways. Moreover, we will also examine response functions making use of the Mittag-Leffler expansion[10,11] which has the advantage that the continuum can be discretized in a natural way. Although the validity of the Mittag-Leffler expansion could only be proved for potentials of finite range, thus excluding the important Coulomb interaction, we will apply it even to proton excitations. We will thus assess numerically the usefulness of this expansion to treat nuclear problems.

To avoid uncertainties resulting from the numerical integration of the Schrödinger equation we will use a model potential for which the solutions can be given in closed analytic form. The convergence properties of the different pole expansions will first be studied in the single-particle case. Neutrons and protons will be treated separately and for different partial waves. With the experience gained in those cases we will calculate particle-hole response functions, where the contribution of all partial waves (for neutrons as well as for protons) may be relevant.

The formalism is presented in Sec. II and the applications for the case of the square well and the square well plus Coulomb potential are presented in Sec. III. A summary and conclusions are given in Sec. IV.

II. FORMALISM

If a nucleus is exposed to an external field f, the response function

$$R(E)=\int d\mathbf{r}\,d\mathbf{r}'f(\mathbf{r})^*G(\mathbf{r},\mathbf{r}';E)f(\mathbf{r}'') \tag{2.1}$$

measures the change of the nuclear density due to its influence. In Eq. (2.1), G is the Green function which describes the propagation of the nuclear system. The strength of the nuclear excitation can be measured by the strength function

$$S(E)=\sum_{n>0}\langle 0|f|n\rangle^2\delta(E-E_n)=-\frac{1}{\pi}\mathrm{Im}R(E)\ , \tag{2.2}$$

where $|n\rangle$ and E_n are the eigenfunctions and energy eigenvalues of the system. The response function $R(E)$ is real below threshold. It has poles on the real energy axis for the bound states and shows a resonant behavior above

threshold whenever the Green function has a complex pole close enough to the real energy axis. Therefore, the influence of the continuum is controlled by the Green function. In the case of particle-hole excitations, the Green function is well described within the RPA, i.e.,

$$G_{ph}(\mathbf{r},\mathbf{r}';E)=G_{ph}^{(0)}(\mathbf{r},\mathbf{r}';E)+\int d\mathbf{r}_1 d\mathbf{r}_2 G_{ph}^{(0)}(\mathbf{r},\mathbf{r}_2;E) \times V_{ph}(\mathbf{r}_1\mathbf{r}_2)G_{ph}(\mathbf{r}_2,\mathbf{r}';E) , \tag{2.3}$$

where V_{ph} is the residual (particle-hole) interaction. $G_{ph}^{(0)}$ is the bare particle-hole Green function corresponding to the Hartree-Fock Hamiltonian H_0 with occupied states ϕ_h and corresponding eigenenergies ϵ_h, i.e.,

$$G_{ph}^{(0)}(\mathbf{r},\mathbf{r}';E) =\sum_h \phi_h^*(\mathbf{r})\left\langle \mathbf{r}\left|\frac{1}{H_0-\epsilon_h-E}+\frac{1}{H_0-\epsilon_h+E}\right|\mathbf{r}'\right\rangle\phi_h(\mathbf{r}') , \tag{2.4}$$

where the two terms between bars are the single-particle Green functions corresponding to the propagation of a particle with energy $\epsilon_p=E+\epsilon_h$ and $\epsilon_p=-E+\epsilon_h$, respectively.

The partial wave expansion for the single-particle Green function is[12]

$$\left\langle \mathbf{r}\left|\frac{1}{H_0-\epsilon_p}\right|\mathbf{r}'\right\rangle=G(\mathbf{r},\mathbf{r}';\epsilon_p) =\frac{2\mu}{\hbar^2 rr'}\sum_{ljm}\mathbf{Y}_{l,j}^m(\hat{r})\mathbf{Y}_{l,j}^{m\,*}(\hat{r})\mathbf{Y}_{l,j}^{m\,*} \times(\hat{r}')g_{lj}(r,r';k) , \tag{2.5}$$

where μ is the reduced mass of the particle. The $\mathbf{Y}_{l,j}^m$ are the vector spherical harmonics. From now on we will drop the l,j indices of the partial Green function g.

The use of a separable residual interaction,[6,13]

$$V_{ph}^{\lambda}(r_1r_2)=-\kappa_\lambda Q_\lambda(\mathbf{r}_1)\cdot Q_\lambda(\mathbf{r}_2) , \tag{2.6a}$$

$$Q_{\lambda\mu}(\mathbf{r})=f_\lambda(r)Y_{\lambda\mu}(\hat{r}) , \tag{2.6b}$$

where the radial dependence of the multipole operator Q coincides with that of the external field f, greatly simplifies the evaluation of the response function (2.1). In this case the response function becomes

$$R(E)=\frac{R^{(0)}(E)}{1+\kappa_\lambda R^{(0)}(E)} , \tag{2.7}$$

where $R^{(0)}$ is the bare response function, i.e., the one corresponding to the Green function $G_{ph}^{(0)}$.

The single-particle Green function can be calculated either exactly or approximately by truncating some spectral representation. The aim of this work is to investigate the practical value of different spectral representations by comparing to the exact results.

A. Representations of the single-particle Green function

For a spherically symmetric potential the exact form of the single-particle Green function (2.5) is

$$g(r,r';k)=-u(r_<)v(r_>)/W , \tag{2.8}$$

where $u(r)$ and $v(r)$ are the regular and the irregular solutions of the single-particle Hamiltonian H_0, and W denotes their Wronskian. The smaller and the larger between r and r' are denoted by $r_<$ and $r_>$, respectively. The boundary conditions for the regular and the irregular solutions are

$$u(r=0)=0 \tag{2.9a}$$

and

$$\lim_{r\to\infty} v(r)=e^{ikr} . \tag{2.9b}$$

The single-particle Green function can also be written in a spectral expansion form, i.e., in terms of the eigenvectors of H_0. The spectrum of a potential well with finite depth contains a finite number of bound states and a continuum of scattering states. In terms of this representation Newton[14] wrote the Green function as

$$g(r,r';k)=\sum_n \frac{w_n(r,k_n)w_n(r',k_n)}{k^2-k_n^2} +\frac{2}{\pi}\int_0^\infty dq\frac{u^{(+)}(r,q)u^{(+)}(r',q)}{k^2+i\epsilon-q^2} , \tag{2.10}$$

where w_n are the wave functions of the bound single-particle states and $u^{(+)}(r,q)$ are scattering states, i.e., they represent the partial wave components of a wave consisting of an incoming plane wave plus an outgoing spherical wave as $r\to\infty$.

One can generalize the definition of "eigenvectors" of the single-particle Schrödinger equation by requiring the boundary conditions[15,16]

$$\lim_{r\to 0} w_n(r,k_n)=0 , \tag{2.11a}$$

$$\lim_{r\to\infty} w_n(r,k_n)=N_n e^{ik_n r} , \tag{2.11b}$$

where k_n is the asymptotic momentum of the state with energy eigenvalue $\mathcal{E}_n$, i.e.,

$$\mathcal{E}_n=\frac{\hbar^2}{2\mu}k_n^2 . \tag{2.12}$$

The eigenvalues $\mathcal{E}_n$ can now be complex. Writing

$$k_n=\kappa_n-i\gamma_n , \tag{2.13}$$

the eigenvectors belonging to those eigenvalues can be classified in four classes, namely: (a) bound states, for which $\kappa_n=0$ and $\gamma_n<0$; (b) antibound states with $\kappa_n=0$ and $\gamma_n>0$; (c) decay resonant states (Gamow resonances) with $\kappa_n>0$ and $\gamma_n>0$; (d) capture resonant states with $\kappa_n<0$ and $\gamma_n>0$. From Eq. (2.11b) one sees that only the bound wave functions do not diverge.

With the standard definition of scalar product

$$\langle w_2|w_1\rangle=\int_0^\infty w_2^*(r,k_2)w_1(r,k_1)dr\ , \tag{2.14}$$

only the bound states can be normalized in an infinite interval. Therefore this definition has to be generalized in order to be able to use the generalized "eigenvectors." This can only be done if one uses a bi-orthogonal basis and apply some regularization method for calculating the resulting integrals. Bi-orthogonality means that in bra position one should use the mirror state $\tilde{w}_n$ instead of w_n, i.e., the solution which corresponds to $\tilde{k}_n=-k_n^*$. As a regularization method we use the complex rotation suggested in Ref. 17, which became later known as exterior complex scaling.[18] Within this method one rotates the radial distance r with a suitable angle only beyond the distance where the nuclear interactions die out. Details on the regularization procedure can be found in Ref. 19.

The representation Eq. (2.10) of the single-particle Green function can be generalized by changing the path of integration, as shown in Fig. 1. The resulting expression, of Berggren,[7] is

$$g(rr';k)=\sum_n \frac{\tilde{w}_n^*(r,\tilde{k}_n)w_n(r',k_n)}{k^2-k_n^2} + \frac{2}{\pi}\int_{L^+}dq\frac{\tilde{u}^*(r,q)u_n(r',q)}{k^2+i\epsilon-q^2}\ , \tag{2.15}$$

where the sum runs over bound states plus the decaying resonant states which lie between the right-hand half of the path L (denoted by L^+) and the real axis in Fig. 1. Although there is not any real physical system without continuum states, the approximation of neglecting the integral contribution to the Green function (2.10) is justified only in the analysis of bound and, in some cases, even quasibound states. Actually, our calculation will clarify this point, as will be seen in the Sec. II B. However, when properties closely linked with the continuum are to be analyzed (e.g., escape widths of giant resonances) the bound representations show their limitations. The advantage of introducing the L contour is that although we neglect the integral in Eq. (2.15), and use only the finite sum of the first term, we still include the most important (from a physical point of view) process occurring in the continuum, i.e., the resonant part. The numerical evaluation of that integral would imply the discretization of the wave number k along the contour L^+ and the solution of the radial equation for each of these complex k values. Although we avoid this formidable task we are able to estimate its effect by taking the difference between the exact results and those obtained within the truncated spectral expansion.

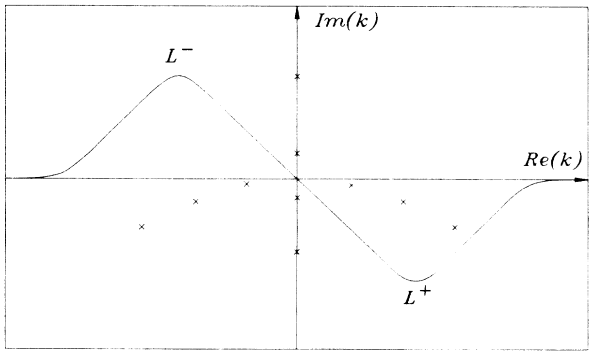

FIG. 1. Integration path L^+ for the single-particle Green function (2.15). The crosses indicate k_n values [Eq. (2.13)] belonging to the outgoing solutions of the Schrödinger equation. They are also poles of the Green function.

In the Berggren expansion of the Green function we then consider only bound states and Gamow resonances as a single-particle representation to describe excitations lying in the continuum. It has been shown that Gamow resonances have large overlaps with certain wave packets centered at the resonance energy.[11] Therefore, the use of Gamow resonances would correspond to the use of wave packets, which is a proper procedure to describe processes in the continuum.

Another representation of the single-particle Green function, which has been presented so far as valid only for central potentials of finite range, is given by the Mittag-Leffler expansion,[10,11] i.e.,

$$g(r,r';k)=\sum_n \frac{w_n(r,k_n)\tilde{w}_n^*(r',\tilde{k}_n)}{2k_n(k-k_n)}\ , \tag{2.16}$$

where the sum now runs over all classes of poles. It only contains a countably infinite set of discrete states, but for practical purposes the series must be truncated and in this way the method becomes an approximate one. If there were some long-range potential in the problem, the truncation to a finite number of states would imply the neglect of the contribution of an integral along a complex contour.[10]

B. Response functions in different representations

Using the standard representation of the Green function given by Eq. (2.8) we will calculate response functions "exactly." We will compare these calculations with those using the Berggren and Mittag-Leffler Green functions. In both cases we will take a limited number of terms in the summations of Eqs. (2.15) and (2.16), respectively. The idea is to probe the convergence as the number of terms in the sum is increased. In the Berggren case we neglect the integral of Eq. (2.15) and, therefore, taking a limited number of terms in the summation may be a drastic approximation even for a potential of finite range. That integral in itself may not be negligible. But we hope that for narrow resonances, i.e., for those lying near the real axis in Fig. 1, the influence of the continuous background (represented by the integral) will be small if the path L^+ is far enough from the physical pole. That is, we assume that the behavior of the response function will be dominated by narrow poles of the Green function in Eq. (2.1). In the case of single-particle response functions, those poles are the resonances of the expansions (2.15) and (2.16). Therefore, in this case, the expansions are expected to converge rapidly. However, for more complex excitations (like particle-hole giant resonances) the individual single-particle resonances might not play a

dominant role. Later we will analyze the single-particle and the particle-hole cases separately.

1. Single-particle response function

For this case the expression of the response function (2.1) is rather straightforward. Labeling by p the set of $\{lj\}$ quantum numbers, and for a field carrying a multipolarity λ, the exact response function is, from Eq. (2.8),

$$R(p;\lambda;E)=-\frac{2\mu}{\hbar^2}\int r\,dr\,r'dr' f_\lambda^*(r)\frac{u_p(r_<)v_p(r_>)}{W}f_\lambda(r'). \tag{2.17}$$

The corresponding expression for the Berggren representation is, from (2.15),

$$R_B(p;\lambda;E)=\frac{2\mu}{\hbar^2}\sum_n \frac{1}{k^2-k_n^2}\int r\,dr\,r'dr' f_\lambda^*(r)w_n(r,k_n)\times w_n(r',k_n)f_\lambda(r'), \tag{2.18}$$

where the relation between E and k is as in Eq. (2.12) (but note that E is the physical energy, i.e., a real quantity in the response functions) and the sum runs over all bound states and Gamow resonances that lie between the real axis and the path L^+ in Fig. 1.

In the same fashion for the Mittag-Leffler (ML) expansion, one obtains, from (2.16),

$$R_{\rm ML}(p;\lambda;E)=\frac{2\mu}{\hbar^2}\sum_n \frac{1}{2k_n(k-k_n)}\int rdr\,r'dr' f_\lambda^*(r)w_n\times(r,k_n)w_n(r',k_n)f_\lambda(r'), \tag{2.19}$$

where the sum runs over all classes of poles of the single-particle Green function (crosses in Fig. 1).

2. Particle-hole response function

In this case the Green function is given by Eq. (2.3). Using a particle-hole separable interaction of the form of Eq. (2.6), the response function becomes as in Eq. (2.7). Therefore, the important quantity is the bare-response function $R^{(0)}$. For a field of multipolarity λ it is

$$R^{(0)}(\lambda;E)=\sum_{ph}|M(ph;\lambda)|^2\int dr\,dr'\phi_h(r)f_\lambda^*(r)[g_p(rr';E+\epsilon_h)+g_p(r'r;-E+\epsilon_h)]\phi_h(r')f_\lambda(r'), \tag{2.20}$$

where p labels the partial waves, h labels the occupied (hole) states, and g_p is the single-particle Green function. The quantity M is

$$M(ph;\lambda)=(-1)^{j_p+1/2}i^{l_p-l_h+\lambda}\hat{j}_p\hat{\lambda}\hat{j}_h\begin{pmatrix} j_p & \lambda & j \\ \frac{1}{2} & 0 & -\frac{1}{2}\end{pmatrix}, \tag{2.21}$$

where the natural parity state condition $(-1)^{l_p+l_h-\lambda}=1$ was used. The exact form for $R^{(0)}$ is obtained by using, in Eq. (2.20), the expression of g_p given by Eq. (2.8), as in the continuum RPA.[12,13] The Berggren form is obtained by using the sum in Eq. (2.15) for g_p, which is the same approximation that leads to the RRPA.[5,6] The Mittag-Leffler form is obtained by using g_p as in Eq. (2.16).

III. APPLICATIONS

A. Square well without and with Coulomb potential

The model we use to test the approximations discussed earlier for neutrons consists of a square well potential of radius a and depth $-V_0$. For protons a Coulomb term Ze^2/r is added to the square well potential for $r>a$. Inside the potential the widely used parabolic shape of the Coulomb potential will be replaced by the constant value Ze^2/a for the sake of simplicity. The value of this constant is included in the numerical value of V_0 for protons.

For neutrons, the radial part of the corresponding single-particle wave function is given by[20]

$$w_{nl}(r)=\begin{cases} rj_l(\kappa r) & \text{for } r\le a \\ r\dfrac{j_l(\kappa a)}{h_l^+(ka)}h_l^+(kr) & \text{for } r>a\end{cases}, \tag{3.1}$$

where $j_l(x)$ and $h_l^+(x)$ are the spherical Bessel and Hankel functions, respectively,

$$\kappa^2=k^2+2\mu/\hbar^2V_0,$$

and k is an in Eq. (2.12) with the complex energies $\mathcal{E}_n$ being solutions of the transcendental equation

$$\left.\frac{dh_l^+(kr)/dr}{h_l^+(kr)}\right|_{r=a}=\left.\frac{dj_l(\kappa r)/dr}{j_l(\kappa r)}\right|_{r=a}. \tag{3.2}$$

For protons the form of Eqs. (3.1) and (3.2) are the same except that for $r>a$ we replace the Hankel functions by the corresponding Coulomb functions.

As our intention is to simulate excitations corresponding to ^{208}Pb, we choose for the potential parameters the values $a=7$ fm and $V_0=45$ (55) MeV for neutrons (protons). With this we calculated the four classes of eigenstates discussed in Sec. II, with eigenvalues $\mathcal{E}=\mathcal{E}_r+i\mathcal{E}_i$ such that $-V_0<\mathcal{E}_r<2000$ MeV and -150 MeV $<\mathcal{E}_i<0$. In Table I we present the lowest 20 neu-

TABLE I. The lowest single-particle states (i.e., with lowest real part of the energy) corresponding to a square well nuclear potential of radius $a=7$ fm, depth $V_0=45$ (55) MeV for neutrons (protons), and $Z=82$. The neutron (proton) energies ϵ_n (ϵ_p) are in MeV. The principal quantum number N corresponding to the harmonic oscillator potential is also given. Note that all imaginary values are negative, as it should be for decaying resonant states.

N	State	ϵ_n	ϵ_p
0	$0s$	-41.51	-51.38
1	$0p$	-37.88	-47.60
2	$0d$	-33.31	-42.83
2	$1s$	-31.16	-40.57
3	$0f$	-27.87	-37.14
3	$1p$	-24.21	-33.25
4	$0g$	-21.59	-30.55
4	$1d$	-16.41	-24.95
5	$0h$	-14.51	-23.09
4	$2s$	-14.48	-22.81
5	$1f$	-7.90	-15.74
6	$0i$	-6.68	-14.79
	i	$-6.13-i1.57$	
5	$2p$	-4.99	-12.19
	g	$-0.35-i4.29$	
6	$1g$	$0.99-i0.00$	-5.68
	h	$1.49-i8.16$	
7	$0j$	$1.85-i0.00$	-5.67
6	$2d$	$3.53-i1.70$	-0.80
6	$3s$	$5.64-i3.37$	$1.09-i0.00$

tron single-particle states, i.e., the 20 bound states and Gamow resonances with the lowest real part of the energy. In addition, the corresponding single-particle states for protons are given. As expected, the Coulomb and centrifugal barriers significantly affect the width of the resonances. The larger the barrier, the smaller the width. In Table I one can associate to each proton state a harmonic oscillator orbit. That is, inside the nuclear volume the wave functions corresponding to Table I have, for a given value of the orbital angular momentum, the same number of nodes as the corresponding harmonic oscillator wave function. This is not surprising because the proton states in Table I are all bound, except the $3s$ state. On the contrary, the neutrons, lacking the Coulomb barrier to bound them, may show low-lying Gamow resonances so wide that their wave functions do not resemble any particular harmonic oscillator wave function. This is exemplified by the three states that do not have any corresponding proton partner in Table I.

1. Single-particle response function

With the wave functions calculated in this way, one can now evaluate the single-particle response functions of Sec. II B 1. We choose for the field f_λ a square barrier of the form

$$f_\lambda(r)=\begin{cases}1 & \text{for } r_0-\delta<r<r_0+\delta \\ 0 & \text{otherwise}\end{cases} \tag{3.3}$$

which resembles the derivative of a Saxon-Woods potential. We performed a number of calculations changing r_0 within reasonable limits around the radius a, and changing δ from 0.1 fm to 1 fm. The calculated response functions do not depend appreciably upon these changes. The results that we present here correspond to $r_0=6.75$ fm and $\delta=0.75$ fm.

The calculation of the exact response function (2.17) is, in this single-particle case, rather straightforward. The corresponding calculations for the Berggren and Mittag-Leffler expansions require us to set a limit on the number of states n in the summations of Eqs. (2.18) and (2.19). In fact, the objective of this calculation is to find which terms of the summation are important and which ones are negligible. In the calculations we use the expression "all terms" meaning all states calculated in the Sec. III A. The set of states used in the Berggren expansion (e.g., Table I) seems to be a natural extension of the shell model basis. Due to this similarity we sometimes call "basis elements" the bound states and resonances used in summations (2.18) and (2.19). Although the important quantity from a physical point of view is the imaginary part of the response function, which is the strength function Eq. (2.2), in most cases we will present the real part as well.

In all cases calculated by us, the response functions (2.17)–(2.19) practically coincide with each other in the resonance region if all terms are included in the Berggren and Mittag-Leffler basis. As an example we present the $l=4$ neutron case in Fig. 2. Within the precision of the scale one cannot distinguish among the three results.

A resonant behavior in the response function (which only depends upon the real energy) implies, from Eq. (2.1), that its behavior is dominated by a pole of the Green function corresponding to a narrow Gamow state. In the case of Fig. 2 that pole is the $1g$ state of Table I with $\mathcal{E}_n=(0.9883-i0.0018)$ MeV. Including only this level in the summations of Eqs. (2.18) and (2.19), one is still not able to distinguish among the results of the exact and approximate calculations in the neighborhood of the resonance. This is perhaps not surprising, since this pole lies very close to the real axis. To test the range of validity of this drastic approximation of including only one term in the Berggren and Mittag-Leffler expansions, we study cases where no single-particle state was dominant. This occurs if the resonances in the response function are wide. We present an example of this type in Fig. 3. Here we neglected all basis elements lying above 80 MeV. The resulting basis consists only of the negative energy states, the sharp resonance $1g$ mentioned above and two broad resonances with energies $(30.20-i7.93)$ MeV and $(71.97-i14.92)$ MeV. The exact result is approximated reasonably well even within this small basis, as seen in Fig. 3.

We found that, in general, it is enough to include only one single-particle state in the basis to reproduce the exact response function in the resonant region. However, for energies between resonances one has to include at least the two basis states lying immediately below and above the energy considered.

As another instructive illustration we present in Fig. 4 the response function corresponding to $l=0$ protons in-

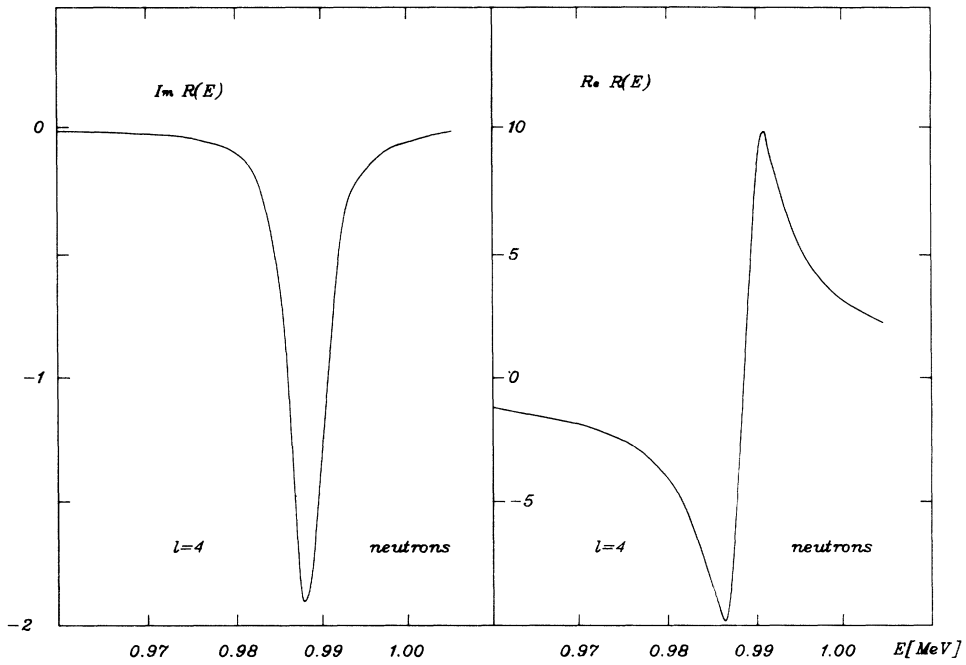

FIG. 2. Imaginary and real part of the $l=4$ neutron single-particle response function (in arbitrary units) for the square well potential $V_0=45$ MeV; $a=7$ fm. The exact response function (2.17), as well as the Berggren and Mittag-Leffler expressions (2.18) and (2.19), including all terms in the summations, are drawn. All curves coincide within the precision of the figure.

cluding all terms in the basis. Again one sees that the agreement between the exact result and the approximate expressions including all terms is excellent. The example of Fig. 4 is also an interesting case because it shows that the Berggren strength function does not vanish below threshold. This indicates that either the integral on the continuous path L of Fig. 1 is important in this region, or that the neglect of the incoming waves produces a wrong behavior of the response function near threshold.

One observes in Fig. 4 that the Mittag-Leffler expansion is working surprisingly well for protons, i.e., for the long-range Coulomb interaction. We found that this

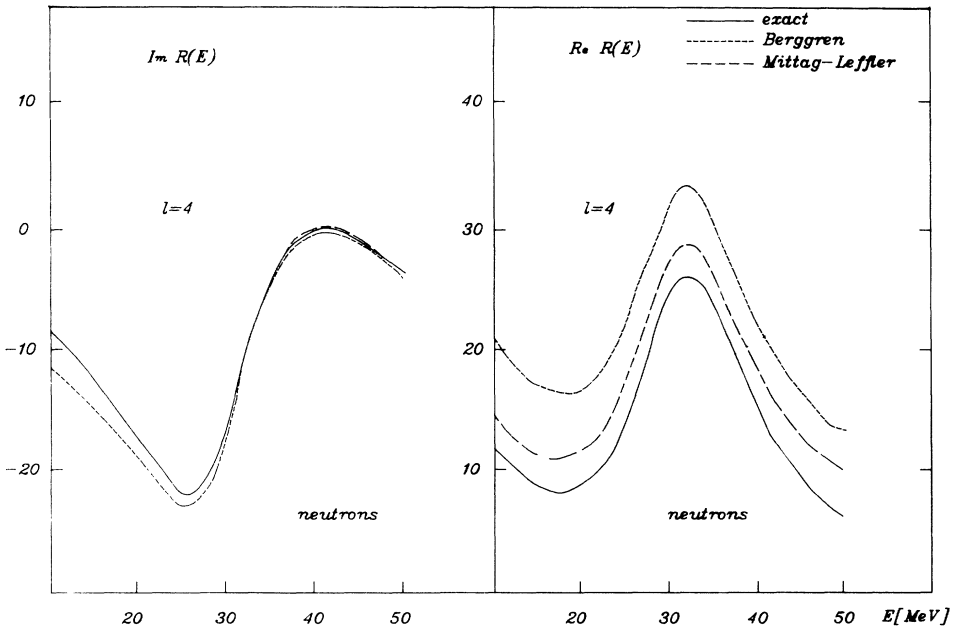

FIG. 3. As in Fig. 2 in the energy range between 10 and 50 MeV. Only the poles with $\mathrm{Re}(\epsilon_n) < 80$ MeV are included in the expansions. For the imaginary part the Mittag-Leffler result almost coincides with the exact one.

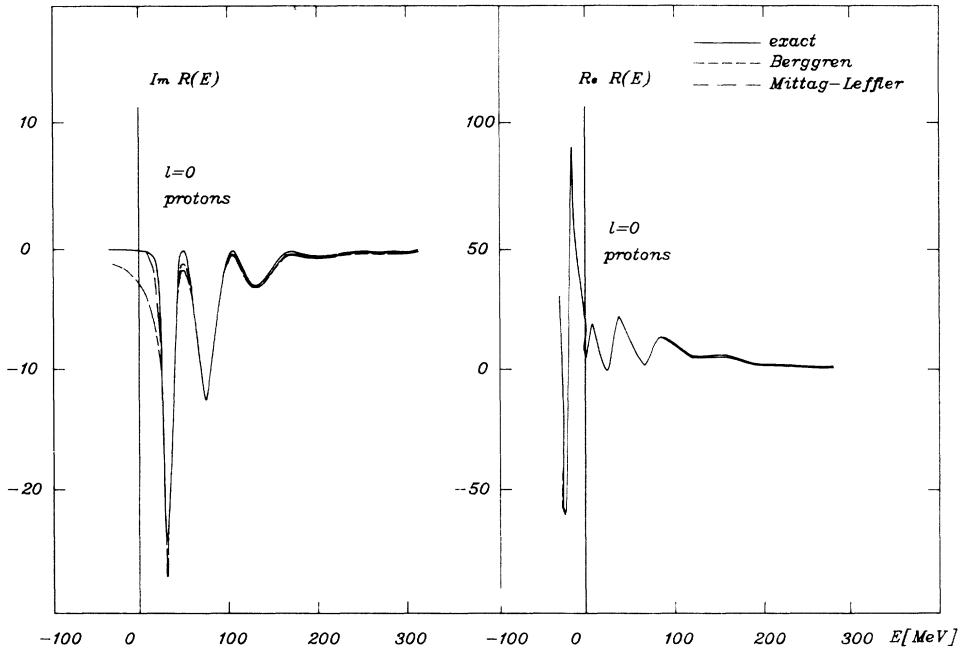

FIG. 4. As in Fig. 2 for $l=0$ protons ($V_0=55$ MeV; $a=7$ fm; $Z=82$).

feature is common to all partial waves that we investigated. This important result is rather unexpected since no analytical proof has so far been found for the validity of the expression (2.16) for a potential of infinite range. The validity of the Mittag-Leffler expansion even for protons opens new possibilities for its application to real nuclei.

The case presented in Fig. 4 is interesting also because in the energy range of Fig. 4 there are several resonances. One can then analyze the influence of a particular basis element upon the different resonances. Thus, in Fig. 5 we included in the expansion only the term corresponding to the first peak. The agreement of both the Mittag-Leffler and the Berggren expansions with the exact result is excellent in the region around that peak. A similar agree-

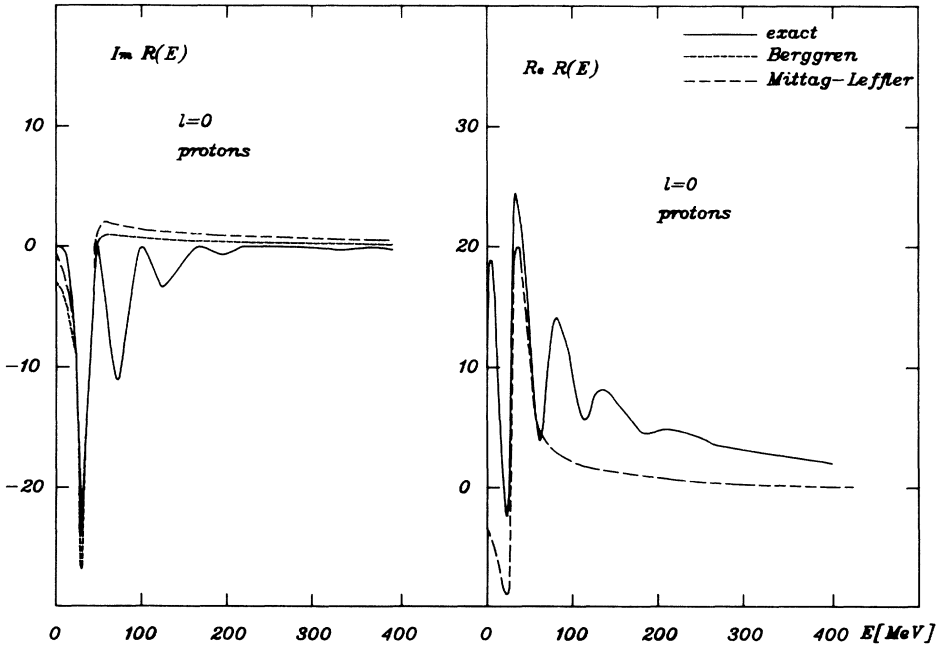

FIG. 5. As in Fig. 4 but including only one element [with energy $\epsilon_n=(29.6-i5.0)$ MeV] in the expansions. For the real part the Mittag-Leffler and Berggren expansions coincide.

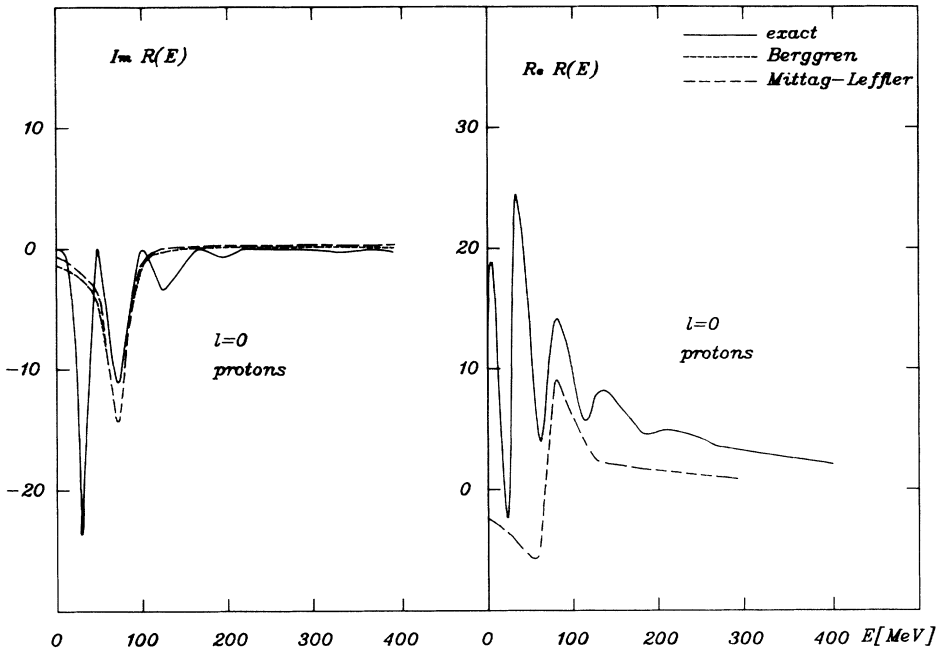

FIG. 6. As in Fig. 5 but including only the resonance with energy $\epsilon_n = (71.2 - i11.6)$ MeV in the expansions. For the real part the Mittag-Leffler and Berggren expansions coincide.

ment is found when including only the terms corresponding to the other peaks, as seen in Fig. 6 for the second one. In Fig. 7 we present the calculated response function when the basis consists of the two terms corresponding to Figs. 5 and 6. One sees that now the exact result is reproduced by the approximated expansions even in the energy region between the two resonances. We have also checked that including the three terms corresponding to the lowest three peaks in Fig. 7, the approximated results agree well with the exact one in the whole energy region below 120 MeV.

One may think that the approximations in the aforementioned examples work so well because $l = 0$ is a very simple case. This is particularly valid for the

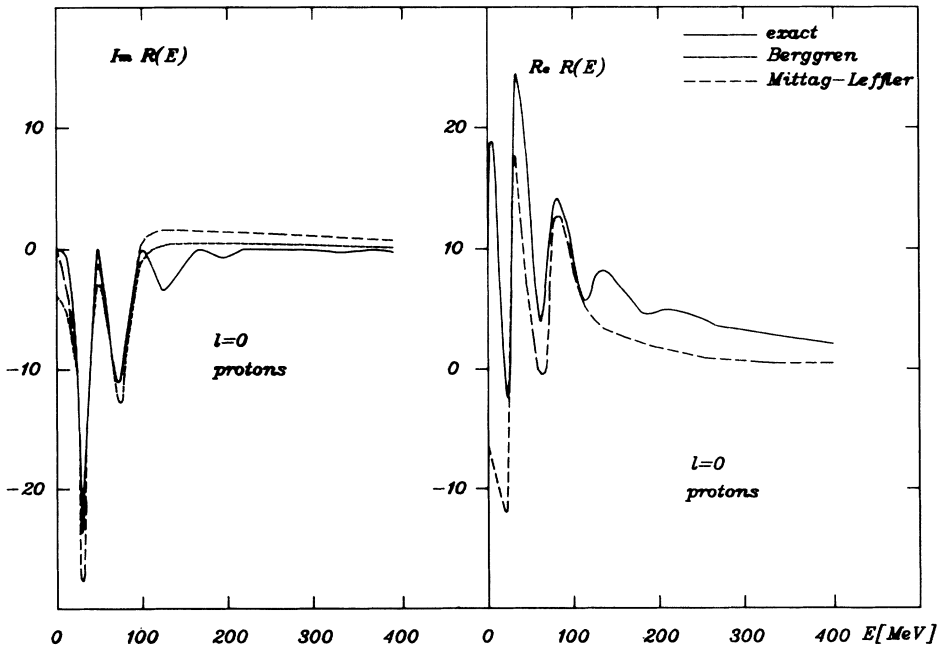

FIG. 7. As in Figs. 5 and 6 but including the two resonances of those figures in the expansions. For the real part the Mittag-Leffler and Berggren expansions coincide.

Mittag-Leffler approximation and its limitations concerning the long range of the interaction. To elucidate this point we present in Fig. 8 the case of $l=5$ protons including the ten lowest basis states. The quality of the agreement among the three calculations is also excellent. Even including only states corresponding to a given peak, one obtains the same quantitative agreements as in the case $l=0$ discussed earlier.

2. *Particle-hole response function*

The single-particle cases studied above may seem to be rather simple since the poles of the Green functions are just the states included in the Berggren and Mittag-Leffler expansions. Therefore, it is not surprising that the resonant behavior of the single-particle response function (which is dominated by those poles) is well approximated even by including only a few terms in the expansions. This feature is not evident in the case of particle-hole excitations, where the correlated poles may be well separated from the corresponding uncorrelated (particle-hole) ones.

To calculate the correlated particle-hole response function we use Eq. (2.7) with the uncorrelated response function as discussed in Sec. II B 2. The strength κ_λ of the separable interaction (2.6) is obtained, as usual, by adjusting its value to fit the energy of the first excited state of angular momentum λ [and parity $(-1)^\lambda$, since only natural parity states feel the separable interaction]. That is, denoting the energy of the yrast state λ by ω_λ, one gets

$$\kappa_\lambda = -1/R^{(0)}(\omega_\lambda) \ . \tag{3.4}$$

Although we have studied several cases corresponding to excitations carrying different angular momenta, we will only present the quadrupole case here because the results of the comparisons, which is the objective of this paper, are the same in all cases.

The single-particle basis consists of the states generated in Sec. III A. The Fermi level was chosen to be the state $2p$ ($2s$) for neutrons (protons) in Table I. Since we are interested in the behavior of the response function in the region of the giant quadrupole resonance ($E<20$ MeV), we found it reasonable to assume an energy of $\omega_2=6.5$ MeV for the yrast quadrupole state in this model calculation. Since $R^{(0)}$ depends upon the approximations done in the calculations, i.e., the expansion used for the Green functions, the value of κ_2 in (3.4) is expected to depend upon those approximations also.

Our single-particle basis has been chosen according to the experience we acquired from the study of the single-particle response. Therefore, we neglected all basis elements lying above 50 MeV. The basis is thus reduced to 47 (45) neutron (proton) states. Since the angular momenta of the hole states are $l<7$ only particle states with $l<9$ enter our quadrupole calculation. With this set of single-particle states one can form $N=219$ uncorrelated particle-hole states, which already represents a drastic truncation of the basis.

Within this basis the values of κ_2 are (in arbitrary units) $\kappa(\text{exact})=0.055$, $\kappa(\text{Berggren})=0.059-i0.005$, and $\kappa(\text{ML})=0.051$, which are rather similar to each other the contrary to aforementioned expectations. Since ω_2 is below the energy threshold, the exact and Mittag-Leffler

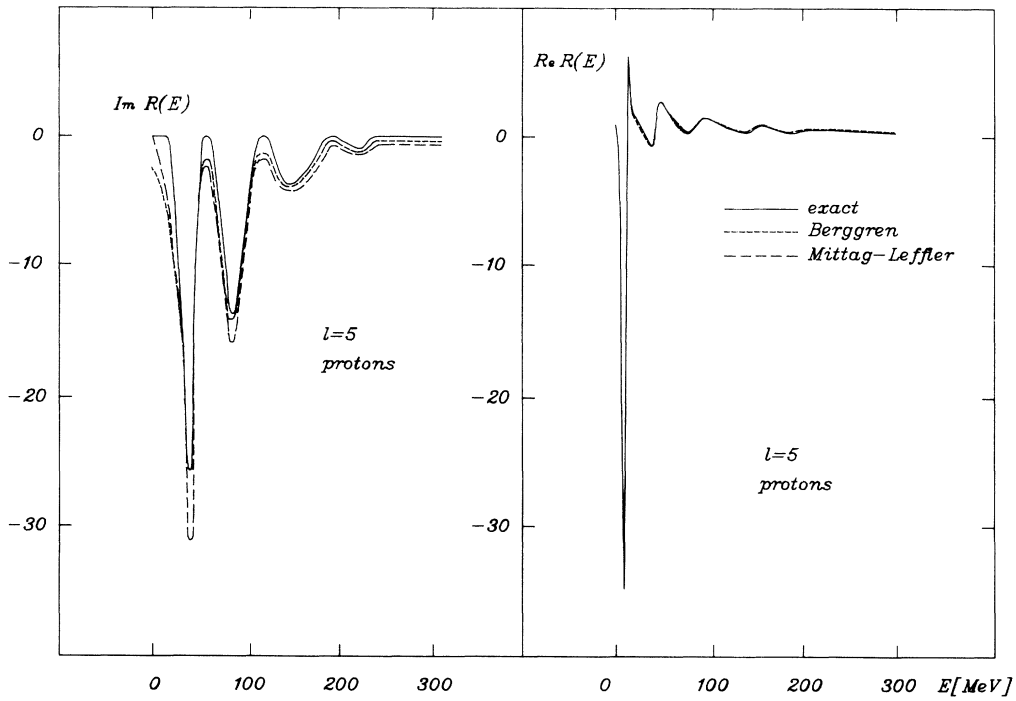

FIG. 8. Imaginary and real part of the $l=5$ proton single-particle response function corresponding to the square well potential $V_0=55$ MeV; $a=7$ fm; $Z=82$. The exact expression (2.17) and the Berggren and Mittag-Leffler expansions (2.18) and (2.19), are given. In the expansions the ten lowest basis states [with $\mathrm{Re}(\epsilon_n)<500$ MeV] have been included.

response functions in Eq. (3.4) (i.e., κ) are real quantities. In the Berggren expansion κ may become complex because one neglects all incoming waves. This feature was also responsible for the wrong behavior of the Berggren response function near the energy threshold.

Using the values of κ given earlier, the exact response function is very similar to the approximated ones in the resonant energy regions. Far from the resonances, however, the Berggren response function differs from the exact one. This is due to spurious contributions given by the small imaginary part of κ(Berggren). We therefore neglect that imaginary part and use κ(Berggren)$=0.059$.

In Fig. 9 we present the strength function calculated within the three expansions. We use a logarithmic scale for $S(E)$ to show in detail the quality of the approximations in the whole range of values of S. In a linear scale the agreement among all curves seems to be artificially better than the one seen in Fig. 9. There is a remarkable agreement between the exact and approximated values of the energy at the center of the resonances. This is an important result because the positions of the complex poles are the quantities of physical interest. These poles are the eigenvalues of the RRPA.[6] Even the shapes of the three curves in Fig. 9 are similar. Near threshold, however, the approximated curves do not follow the exact one. The Berggren strength function even fails to vanish below the threshold energy, i.e., 13.54 MeV. This, again, is a result of the approximated treatment of the continuum background, especially in the Berggren expansion.

We found that wide basis states do not affect the position of the calculated resonances neither in the Berggren nor in the Mittag-Leffler approximation. This feature can again be understood from the expression of the response function (2.1). The poles of the Green function with large imaginary parts are far from the real energy axis and their influence is therefore negligible in the resonance region. One can then truncate the basis further if one is only interested in the resonant behavior of the response function. As an example we show, in Fig. 10, the strength function calculated within the Berggren approximation using a basis consisting of the 37 (35) lowest neutron (proton) single-particle states. This neglects the highest lying broad resonances in the basis used in Fig. 9. The dimension of the resulting particle-hole basis is $N=136$. The corresponding strength function is labeled "restricted" in Fig. 10. For comparison, both the exact and the Berggren calculation of Fig. 9, labeled "full" in Fig. 10, are also shown in Fig. 10. As expected, Fig. 10 shows that wide basis states considerably influence the background, but they play a minor role in the determination of the position of the resonances. The corresponding results for the Mittag-Leffler expansion above threshold are, using the restricted basis, practically the same as the ones obtained with the full basis.

One then concludes that the positions of the poles of the Green function corresponding to narrow resonances are well determined within a basis consisting of narrow elements. A similar conclusion was reached in Ref. 6 by

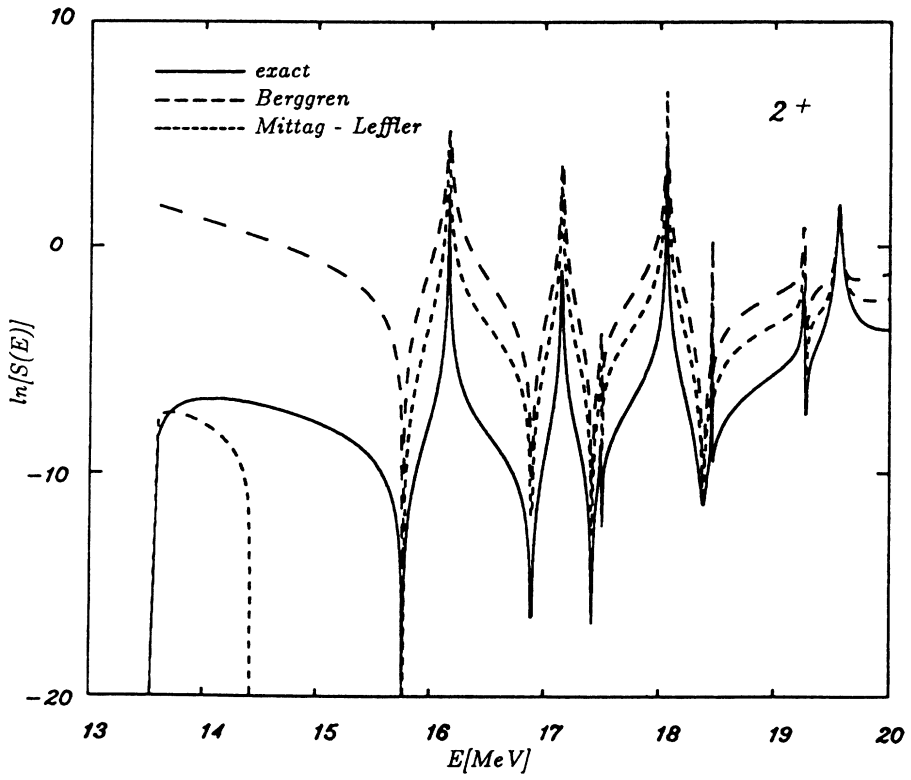

FIG. 9. Quadrupole particle-hole strength function (in arbitrary units) calculated exactly and within the Berggren and Mittag-Leffler expansions.

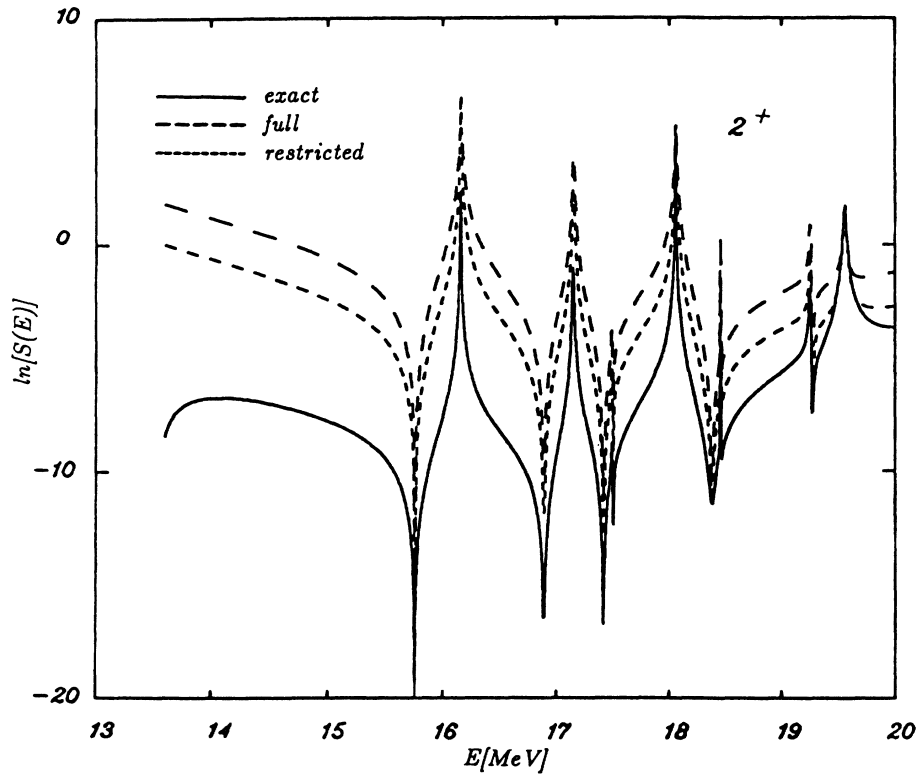

FIG. 10. Quadrupole strength function (in arbitrary units) calculated exactly and within the Berggren expansion using the basis of Fig. 9 ("full") and with the truncated basis discussed in the text ("restricted").

studying the dependence of the complex resonance energies upon the truncation of the RRPA basis. This explains why calculations done within bound (e.g., harmonic oscillator) representations have been so successful in predicting the position of giant resonances,[21] since it is only narrow resonances which can be detected experimentally (note that "narrow" here means small *escape* width).

Finally, it is important to point out that the use of pole expansions considerably reduces the computational time needed to find the resonances in the response function. In the case of the full basis, which is the one that takes the longest time, the pole expansion calculation was 26 times faster than the continuum RPA in a VAX/8650 computer.

IV. SUMMARY AND CONCLUSIONS

The numerical evaluation of nuclear processes which take place in the continuum is an old problem which has not yet been fully solved. To deal with this problem we have studied, in this paper, different approximations where the continuum is replaced by a discrete set of states. The numerical difficulties are thus greatly simplified and, in addition, one gains some physical insight into the physical process by just using the discrete expansion.

To avoid uncertainties related to the numerical solution of the Schrödinger equation, we considered the well-known case of a square well potential, including the long-range Coulomb interaction which can be solved analytically and yet is rather close to the potential felt by nucleons in a nucleus. Using this as a model we studied response functions corresponding to single-particle and particle-hole excitations. The exact evaluation of the response functions was performed by using the exact form of the Green function (2.8). We then evaluated the Green function by using two different pole expansions. In one of them[7] one writes the Green function as a sum plus an integral along a complex path, as shown in Fig. 1. The terms in the sum have singularities which are the poles of the Green function lying between the integration path and the real k axis. These poles correspond to the complex solutions of the Schrödinger equation with regular boundary conditions at the origin and outgoing waves at infinity (Gamow states), as seen in Eq. (2.15). In the applications of this expansion we neglect the integral and include only a limited number of terms in the summation. We call this form of the Green function the "Berggren expansion." The idea behind the Berggren expansion is that the physical resonances, i.e., those which can be seen in the response function, are narrow. Therefore, if one chooses the integration path far enough from the real axis, its contribution would only affect the continuum background. The attractive feature of the Berggren expansion is that it provides a set of linear equations for the complex energies of the particle-hole resonances in a way similar to the RPA. The resulting formalism was called

the resonant RPA in Ref. 6. The similarities between the Berggren formalism and the one corresponding to real (bound) representations is also reflected in the level scheme corresponding to the set of single-particle states used in the Berggren expansion, as seen in Table I. These suggestive similarities induced us to view the Berggren set of states as a "representation" which is a generalization of the shell model basis. The drawback of the Berggren expansion is that it only includes outgoing waves and, therefore, has a wrong behavior below threshold.

In the other expansion[10,11] (Mittag-Leffler) one also writes the Green function as an infinite sum of terms corresponding to all possible solutions of the Schrödinger equation satisfying the boundary conditions (2.11), as seen in Eq. (2.16). There is not any integral contribution to the Mittag-Leffler expansion, which is a great convenience. But its validity has been proved only for potentials of a finite range, thus excluding the important Coulomb potential.

We applied the Berggren and Mittag-Leffler expansions to calculate single-particle and particle-hole response functions. For the single-particle case we found that the results of these two expansions agree very well with the corresponding exact results if a large number of terms is used in the expansions. This may not be surprising since the resonant part of the response function is determined by its complex poles. Actually, in this rather simple case of single-particle excitations, one expects that the inclusion of only relevant terms, i.e., those with poles close to the resonances, would be enough to describe the response function in the neighborhood of the resonances. We found that even using only one term in the expansions, one obtains excellent agreement with the exact result in the resonant region. In these calculations we also found that the Mittag-Leffler expansion reproduces the exact results for neutrons as well as for protons. This is numerical proof of the validity of this expansion for the long-range Coulomb interaction. New possibilities are thus available for the application of the Mittag-Leffler expansion to nuclear problems where the continuum plays a role.

We performed the analysis of particle-hole response functions by using the continuum RPA.[12] In the corresponding Berggren and Mittag-Leffler approximations we used the single-particle propagator as in the single-particle case above. One important objective of our approximate calculation was to investigate the possibility of obtaining the energies of the resonances fast and with reasonable accuracy. Therefore, from the outset we used a very limited number of terms in the expansions. To decide which should be taken into account, we profited from the experience gained in the studies of the single-particle cases. The good agreement between the exact result and the approximations for those cases indicated that, for the particle-hole excitations, it would be enough to consider only terms in the expansions which would be close (in energy) to the resonant region. This is actually the shell model procedure to choose the basis. Using only the lowest 47 (45) single-particle neutron (proton) states in the expansions, we obtained good agreement between the approximations and the exact results as seen in Fig. 9. Even reducing the basis further, the agreement is good in the resonant region as seen in Fig. 10. As in the aforementioned single-particle case, the approximations work very well in the resonant region, however, the background is not well reproduced. This explains why the approximated response functions have the same shapes as the exact one, but the absolute value is different. The computational time is sharply reduced by using the approximate methods.

In conclusion, we have shown in this paper that both the Berggren and Mittag-Leffler expansions are powerful tools to treat nuclear processes taking place in the continuum. This is especially the case for the Mittag-Leffler expansion, which we have shown to be valid for the long-range Coulomb interaction.

Discussions with J. Bang, T. Berggren, E. Maglione, and N. Van Giai are gratefully acknowledged.

[1]S. Yoshida and S. Adachi, Z. Phys. A **325**, 441 (1986).
[2]Ph. Chomaz, Nguyen Van Giai, and S. Stringari, Phys. Lett. B **189**, 375 (1987).
[3]S. Brandenburg, W. T. A. Borghols, A. G. Drentje, L. P. Ekström, M. N. Harakeh, A. van der Woude, A. Hakanson, L. Nilsson, N. Olsson, M. Pignanelli, and R. De Leo, Nucl. Phys. **A466**, 29 (1987).
[4]Nguyen Van Giai, P. F. Bortignon, F. Zardi, and R. Broglia, Phys. Lett. B **199**, 155 (1987); A. Bracco, J. R. Beene, N. Van Giai, P. F. Bortignon, F. Zardi, and R. A. Broglia, Phys. Rev. Lett. **60**, 2603 (1988).
[5]T. Vertse, P. Curutchet, O. Civitarese, L. S. Ferreira, and R. J. Liotta, Phys. Rev. C **37**, 876 (1988).
[6]P. Curutchet, T. Vertse, and R. J. Liotta, Phys. Rev. **39**, 1020 (1989).
[7]T. Berggren, Nucl. Phys. **A109**, 265 (1968).
[8]G. Có and S. Krewald, Nucl. Phys. **A333**, 392 (1985).
[9]B. Buck and A. D. Hill, Nucl. Phys. **A95**, 271 (1967).
[10]J. Bang, F. A. Gareev, M. H. Gizzatkulov, and S. A. Gonchanov, Nucl. Phys. **A309**, 381 (1978); N. Elander, C. Carlsund, P. Krylstedt, and P. Winkler, in *Resonances*, Vol. 325 of *Lectures Notes in Physics*, edited by E. Brändas and N. Elander (Springer-Verlag, New York, 1989), p. 383.
[11]W. J. Romo, Nucl. Phys. **A398**, 525 (1983).
[12]S. Shlomo and G. Bertsch, Nucl. Phys. **A243**, 507 (1975).
[13]S. Yoshida and S. Adachi, Nucl. Phys. **A457**, 84 (1986).
[14]R. G. Newton, *Scattering Theory of Waves and Particles* (McGraw-Hill, New York, 1966), p. 368.
[15]W. J. Romo, Nucl. Phys. **A419**, 333 (1984).
[16]Y. B. Zel'dovich, Sov. Phys.—JETP **12**, 542 (1961).
[17]B. Gyarmati and T. Vertse, Nucl. Phys. **A160**, 573 (1971).
[18]B. Simon, Phys. Lett. **73A**, 211 (1979).
[19]T. Vertse, P. Curutchet, and R. J. Liotta, in *Resonances*, Vol. 325 of *Lectures Notes in Physics*, edited by E. Brändas and N. Elander (Springer-Verlag, New York, 1989), p. 179.
[20]A. Messiah, *Quantum Mechanics* (North-Holland, Amsterdam, 1975), Vol. II.
[21]K. Goeke and J. Speth, Annu. Rev. Nucl. Sci. **32**, 65 (1982).